

1 **Supplementary information**

2 **Direct imaging of the nitrogen rich edge in monolayer**  
3 **hexagonal boron nitride and Its Band Structure Tuning**

4

5 Peizhi Liu<sup>1</sup>, Huifeng Tian<sup>2</sup>, Wolfgang Windl<sup>3</sup>, Gong Gu<sup>4</sup>, Gerd Duscher<sup>5,6</sup>, Yucheng Wu<sup>1</sup>,  
6 Min Zhao<sup>1</sup>, Junjie Guo<sup>1\*</sup>, Bingshe Xu<sup>1\*</sup>, Lei Liu<sup>2\*</sup>

7 1. Key Laboratory of Interface Science and Engineering in Advanced Materials, Ministry  
8 of Education, Taiyuan University of Technology, Taiyuan 030024, China

9 2. Department of Materials Science and Engineering, College of Engineering, Peking  
10 University, Beijing 100871, China

11 3. Department of Materials Science and Engineering, Ohio State University, Columbus,  
12 OH 43210, United States

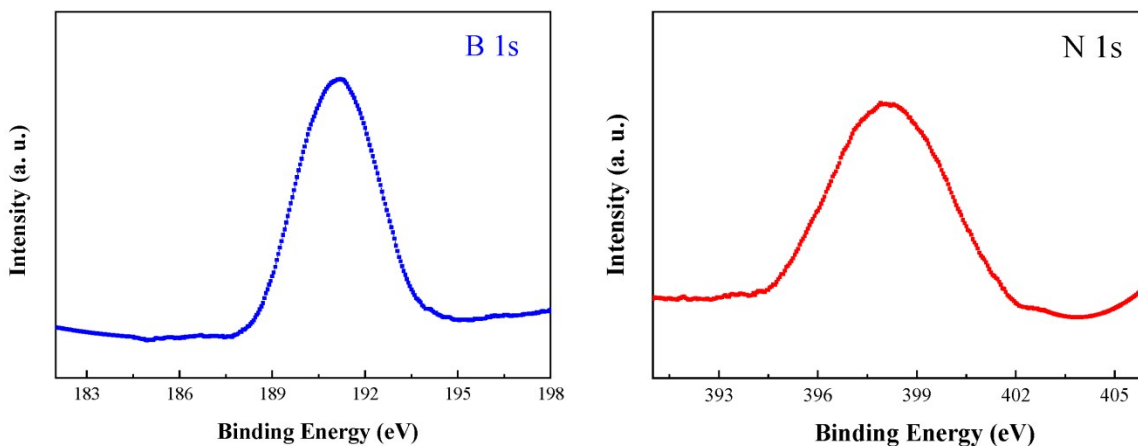
13 4. Department of Electrical Engineering and Computer Science, the University of  
14 Tennessee, Knoxville, Tennessee 37996, USA

15 5. Department of Materials Science and Engineering, the University of Tennessee,  
16 Knoxville, TN 37996, USA

17 6. Materials Science and Technology Division, Oak Ridge National Laboratory, Oak  
18 Ridge, Tennessee 37831, USA

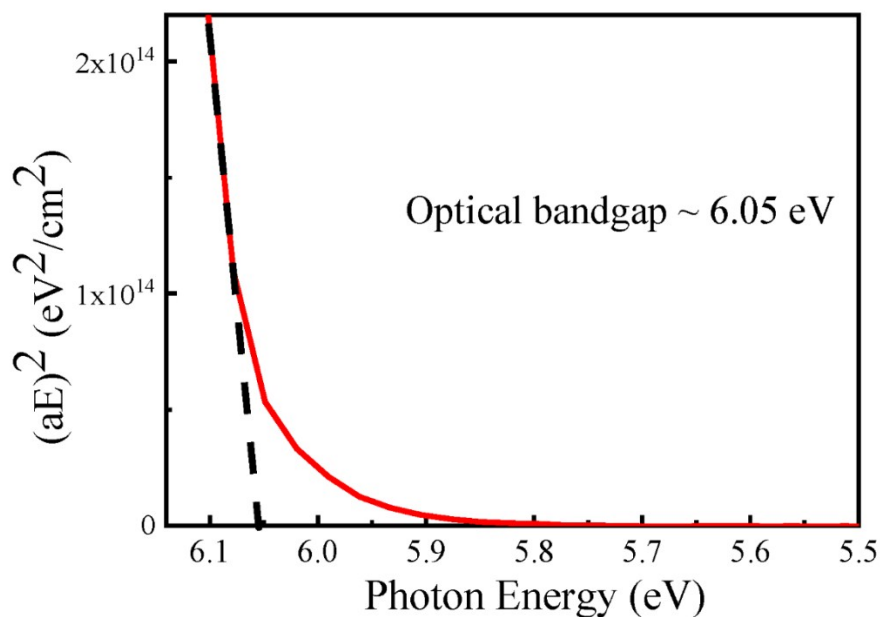
19

20 \*Corresponding author. Email: [guojunjie@tyut.edu.cn](mailto:guojunjie@tyut.edu.cn) (J. G.); [xubs@tyut.edu.cn](mailto:xubs@tyut.edu.cn) (B. X.);  
21 [leiliu1@pku.edu.cn](mailto:leiliu1@pku.edu.cn) (L. L.)



1

2 **Fig. S1. XPS characterization of CVD grown h-BN.** The binding energies of B 1s and  
 3 N 1s state are 191.2 eV and 398.3 eV respectively, indicating the  $sp^2$  bonding and  
 4 therefore the hexagonal phase of BN sheets<sup>1</sup>.

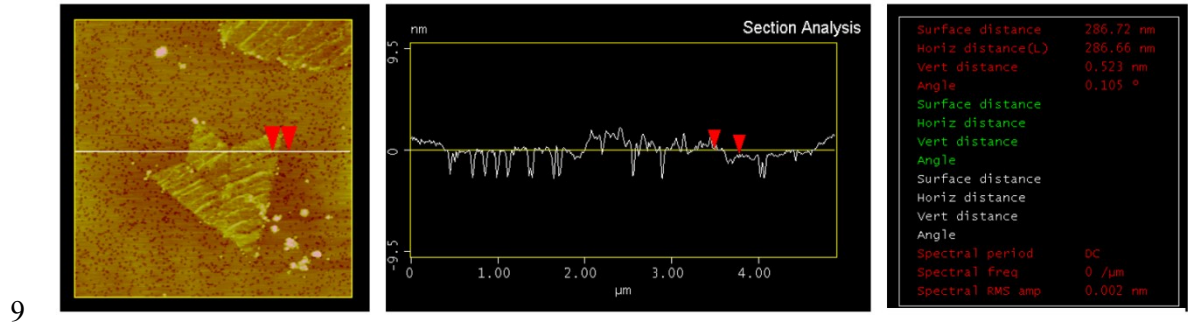


5

6 **Fig. S2. Bandgap measurement of BN crystallites with ultraviolet-visible absorption**  
 7 **spectra.** The extrapolation of the linear part of the  $(\alpha E)^2 - (E - E_g)$  plot intersect X-  
 8 axis at 6.05 eV.

1 Ultraviolet-visible absorption spectra were applied to measure the bandgap of h-BN.  
 2 For direct bandgap semiconductors, the absorption coefficient  $\alpha$  is proportional to  
 3  $\sqrt{(E - E_g)}/E$ , where  $E$  is the incident photon energy and  $E_g$  the optical bandgap<sup>2</sup>. Thus  
 4 the curve of  $(\alpha E)^2$  vs  $(E - E_g)$  can be used to determine the bandgap of h-BN. The  
 5 extrapolation of linear part of the curve intersected X-axis at 6.05 eV, which is the  
 6 bandgap of h-BN, and the measurement is consistent with our HSE06 calculation result  
 7 of 5.91 eV.

8

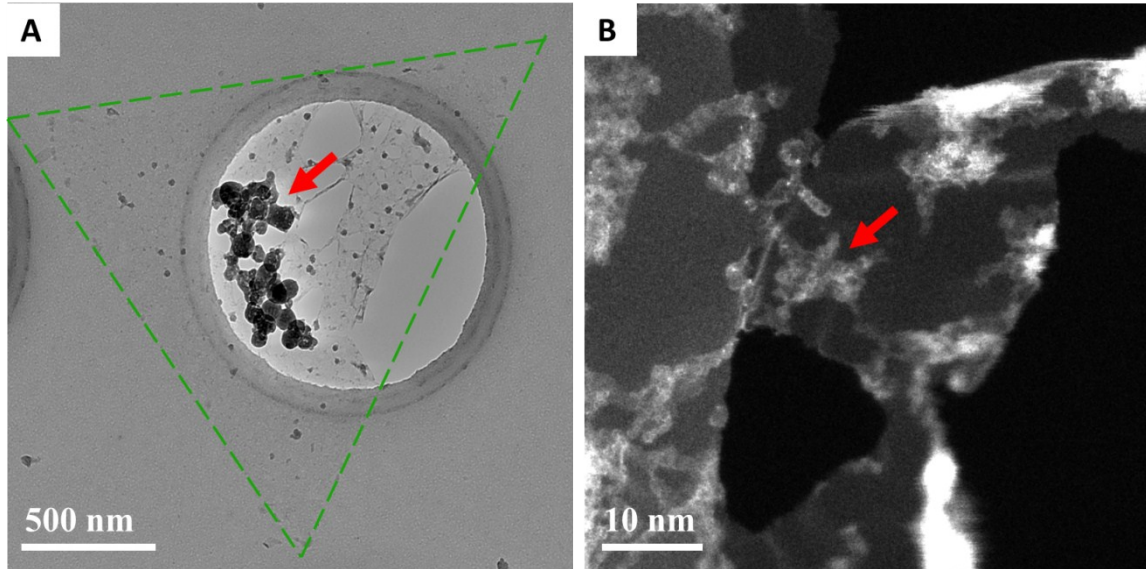


10 **Fig. S3. AFM characterization of single layer h-BN.** CVD grown h-BN domains  
 11 transferred on a silicon wafer was characterized with atomic force microscopy, and the  
 12 vertical distance of 0.523 nm between the edge of an h-BN domain and the substrate  
 13 (denoted with the 2 red markers on the AFM image and the line profile across the  $\mu\text{m}$ -  
 14 size h-BN domain) indicates that the h-BN domain is a monolayer.

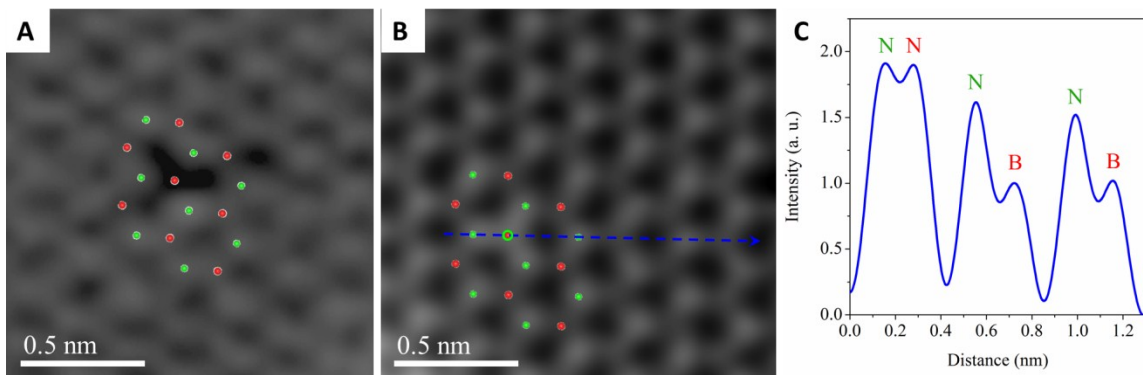
15

16

17



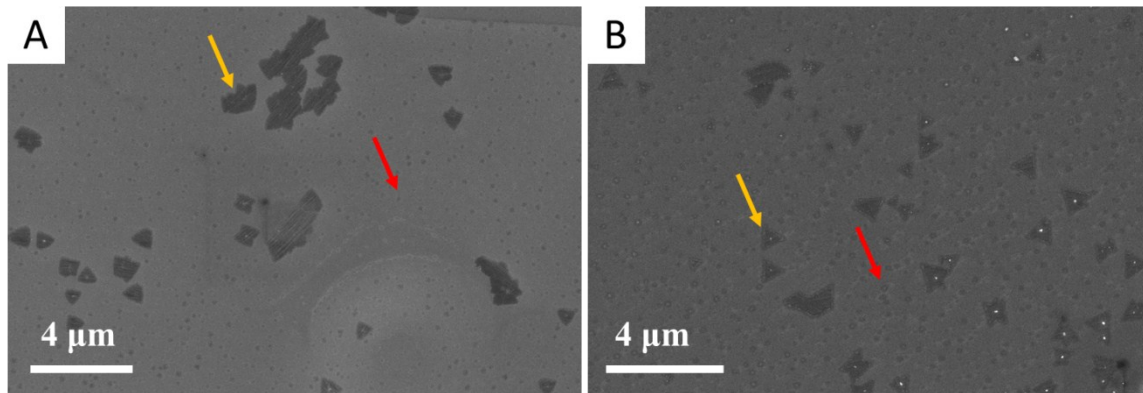
1  
2 **Fig. S4. h-BN monolayer on TEM grid.** (A) An overview of a triangular h-BN  
3 monolayer suspending on a hole of a gold Quantifoil TEM grid. Edges of the triangular  
4 h-BN flake are highlighted with dashed green line in this TEM image. (B) A zooming in  
5 STEM image of the suspended h-BN flake, on which a triangular hole and clean edges  
6 can be observed. Red arrows denote junks on the h-BN monolayer.



7  
8 **Fig. S5. Native defects in h-BN monolayer.** (A) MAADF image of a boron vacancy  $V_B$   
9 in h-BN monolayer. Lattice positions near the defect are overlaid with h-BN atomic  
10 models for visual guidance. Green and red spots represent N and B atoms respectively,  
11 and a red spots in the center of the black tripod hole shows the missing of a B atom. (B)  
12 MAADF image of a nitrogen anti-site  $N_B$  in h-BN monolayer. The red spot with green  
13 outline represents the  $N_B$ . (C) The intensity profile along the blue arrow in (B), convinces  
14 that a boron atom on B site was substituted by a N atom.

1 A defect free h-BN monolayer can sustain a long time scan under a 60 keV electron  
2 beam and gives a high quality atomic resolution images. However, intrinsic defects in h-  
3 BN will cause unstable and thus holes are common to be created under a focused electron  
4 beam. Boron vacancy  $V_B$  is one of the sources of producing holes in h-BN, and Fig. S5A  
5 is a  $V_B$  captured under our low dose MAADF imaging. The overlaid atomic model  
6 demonstrates an absence of B, leaving a dark tripod shape in the h-BN monolayer, which  
7 is the same configuration as the exit-wave reconstructed image of an aberration corrected  
8 HRTEM observation<sup>3</sup>. Nitrogen anti-site  $N_B$  in h-BN monolayer is shown in Fig. S5B. h-  
9 BN atomic structure model on top of the image demonstrates atomic positions of B and N  
10 clearly, and  $N_B$  is denoted as the red dots with green outline. A line profile of image  
11 intensity along B-N bond (blue line with an arrow end in Fig. S5B) was plot and shown  
12 in Fig. S5C. The profile conformed that at this site boron was substituted by nitrogen and  
13 thus N-N couple gives a higher intensity due to the stronger electron scattering possibility  
14 of nitrogen than that of boron.

15



16

17 **Fig. S6. SEM images of nanosized h-BN islands prepared by the bottom-up CVD**  
18 **growth.** (A) and (B) shows the typical SEM images of morphologies of h-BN islands  
19 grown with the duration of less than 1 minute. Small h-BN islands with the lateral size of  
20 sub-100 nm and  $\mu m$ -size h-BN monolayer domains are marked with red and orange  
21 arrows, respectively.

22 With the cold-wall furnace system, the CVD growth with the duration of less than 1  
23 min has been performed, giving rise to the small h-BN islands (marked by the red arrows)

1 with the lateral size of sub-100 nm. Also, the h-BN monolayer domains with larger sizes  
2 ( $\sim \mu m$ ) have been observed and highlighted by orange arrows.

3

4

## 5 **References**

6 1. T.H.Yuzuriha and D.W.Hess, *Thin Solid Films*, 1986,**140**, 199-207.

7 2. X. Blase, Angel Rubio, Steven G. Louie, and Marvin L. Cohen, *Phys. Rev. B*, **51**,  
8 6868.

9 3. C. H. Jin, F. Lin, K. Suenaga and S. Iijima, *Phys. Rev. Lett.*, 2009, **102**, 195505.

10

11

12